Study of the Dissolution of Thin Films of Cerium Oxide by Using a GaPO4 Crystal Microbalance

ARTICLE *in* ANALYTICAL CHEMISTRY · JULY 2009

Impact Factor: 5.64 · DOI: 10.1021/ac900826u · Source: PubMed

6 AUTHORS, INCLUDING:

Sandrine Jakab-Costenoble
Atomic Energy and Alternative Energies Co…
4 PUBLICATIONS **70** CITATIONS
SEE PROFILE

Sébastien Picart
Atomic Energy and Alternative Energies Co…
25 PUBLICATIONS **143** CITATIONS
SEE PROFILE

Anal. Chem. **2009,** *81,* 5139–5145

Study of the Dissolution of Thin Films of Cerium Oxide by Using a $GaPO_4$ Crystal Microbalance

Sandrine Jakab,*,†,‡ Sébastien Picart,*,† Bernard Tribollet,‡ Philippe Rousseau,‡ Hubert Perrot,‡ and Claude Gabrielli‡

CEA, DEN, DRCP, SCPS, LCA, F-30207 Bagnols-sur-Cèze, France, and Université Pierre et Marie Curie, UPR 15 du CNRS-LISE, 4 Place Jussieu, 7552 Paris, France

In this study, microbalance measurements with a $GaPO_4$ crystal were performed to determine the dissolution rate of cerium oxide thin films at room temperature after a high temperature treatment of the hydroxide precursor $Ce(OH)_4$ at 700 °C. The properties of the $GaPO_4$ crystal enables gravimetric measurements to be performed after being heated at high temperatures where the classical quartz crystal microbalance irreversibly loses all its piezoelectric properties. The $GaPO_4$ resonators were calibrated at room temperature by galvanostatic copper deposition before and after a high-temperature treatment, and the sensitivity coefficients K_S were found to be identical, which proved the high potential of $GaPO_4$ at high temperatures. However the accuracy of the gravimetric measurements is lower after a high temperature treatment. The rate determining step of the cerium oxide dissolution seems to be the reduction reaction of Ce(IV) to Ce(III), which is carried out by the hydrogen peroxide present in the dissolution medium.

Cerium oxide (CeO_2) has broad applications in industry. For example, CeO_2 has been utilized as a catalytic support material in engine exhaust gases systems[1] because of its high oxygen ion conductivity and as an electrolyte in solid oxide fuel cells.[2] In addition, in the nuclear research industry, cerium oxide is used to simulate radioactive material behaviors[3] such as PuO_2 in test experiments because of the similarity of their valence charge and their ionic radii.

There are various techniques used to produce cerium oxide films: sputtering,[4] chemical vapor deposition,[5] or sol−gel deposition.[6] Previous works have already studied the deposition of CeO_2 by electrochemical methods.[7,8] In our case, the cathodic deposition seemed to be the most attractive method for the fabrication of CeO_2, because of its high purity and its well controlled film thickness. Actually, hydrous cerium oxide $Ce(OH)_4$ formed from Ce(III) salt solutions was used as a precursor, and a high temperature treatment around 700 °C was necessary to complete the formation of cerium oxide CeO_2.

CeO_2 dissolution studies have been poorly described in the literature,[9,10] despite CeO_2 can be depicted as an oxide model for the study of refractory mineral materials. Moreover, no work has been done on the dissolution of thin films of CeO_2. The quartz crystal microbalance (QCM) has been widely used in the investigation of various electrode processes.[11−13] In particular, this mass-sensitive device has become a suitable method for the investigation of the dissolution kinetics of thin metal films[14−16] and polymers.[17] However, for most of these QCM experiments, the resonators were used around room temperature where the temperature effect on the microbalance frequency can be neglected[18] thanks to the particular cut of the quartz crystal generally used, the well-known single rotating AT-cut. In fact, the absolute limit temperature for the microbalance measurements with a quartz crystal is the Curie point at 573 °C. The quartz crystal irreversibly loses all its piezoelectric properties above this point, and so it does not recover them even when the temperature decreases to room temperature. So a high temperature treatment cannot be considered with a quartz crystal microbalance.

Few solutions were considered to resolve quartz resonator instabilities occurring at high temperature. An original technique was developed by Mecea and Carlsson[19] where the effect of the temperature on the piezoelectric properties up to 570 °C were

* To whom correspondence should be addressed. E-mail: sandrine.jakab@cea.fr (S.J.); sebastien.picart@cea.fr (S.P.).
† CEA, DEN, DRCP, SCPS, LCA.
‡ Université Pierre et Marie Curie.

(1) Bekyarova, E.; Fornasiero, P.; Kaspar, J.; Graziani, M. *Catal. Today* **1998**, *45*, 179–183.
(2) Inaba, H.; Tagawa, H. *Solid State Ionics* **1996**, *83*, 1–16.
(3) Kim, C.-W.; Wronkiewicz, D. J.; Finch, R. J.; Buck, E. C. *J. Nucl. Mater.* **2006**, *353*, 147–157.
(4) Papaiacovou, P. P.; Hussey, R. J.; Mitchell, D. F.; Graham, M. J. *Corros. Sci.* **1990**, *30*, 451.
(5) Pollard, K. D.; Jenkins, H. A.; Puddephatt, R. J. *Chem. Mater.* **2000**, *12*, 701.
(6) Czerwinski, F.; Szpunar, J. A. *Thin Solid Films* **1996**, *289*, 213.
(7) Zhitomirsky, I.; Petric, A. *Mater. Lett.* **1999**, *40*, 263.
(8) Li, F.-B.; Thompson, G. E. *J. Electrochem. Soc* **1999**, *146*, 1809.
(9) Juillet, F.; Adnet, J. M.; Gasgnier, M. *J. Radioanal. Nucl. Chem.* **1997**, *224*, 137–143.
(10) Joret, L.; Cote, G.; Bauer, D. *Hydrometallurgy* **1997**, *45*, 1–12.
(11) Ward, M. D.; Buttry, D. A. *Science* **1990**, *249*, 1000–1007.
(12) O'Sullivan, C. K.; Guilbault, G. G. *Biosens. Bioelectron.* **1999**, *14*, 663.
(13) Buttry, D. A.; Ward, M. D. *Chem. Rev.* **1992**, *92*, 1355–1379.
(14) Hinsberg, W. D.; Wilson, C. G.; Kanazawa, K. K. *J. Electrochem. Soc.* **1986**, *133* (7), 1448.
(15) Roka, A.; Varga, I.; Inzelt, G. *Electrochim. Acta* **2006**, *51*, 6243–6250.
(16) Lukaszewski, M.; Czerwinski, A. J. *Electroanal. Chem.* **2006**, *589*, 38–45.
(17) Hussain, Y.; Wu, Y.-T.; Ampaw, P.-J.; Grant, C. S. *J. Supercrit. Fluids* **2007**, *42*, 255–264.
(18) Cassiède, M.; Pauly, J.; Milhet, M.; Rivaletto, M.; Marrucho, I. M.; Coutinho, J. A. P.; Daridon, J.-L. *Meas. Sci. Technol.* **2008**, *19*, 065704.
(19) Mecea, V. M.; Carlsson, J. O.; Bucur, R. V. *Sens. Actuators* **1996**, *A53*, 371.

10.1021/ac900826u CCC: $40.75 © 2009 American Chemical Society
Published on Web 06/04/2009

decreased by working with a differential measuring system based on a dual resonator. Rahtu and Ritala[20] found a fitting function for modeling the drift of the QCM due to temperature effect at 450 °C. Lastly, Gabrielli et al.[21] used a heated quartz microbalance, using the Joule effect through electrodes deposited on one side of the quartz resonator, in order to simulate scaling of hot pipes at 55 °C.

Nevertheless, these solutions are complicated and do not allow the quartz crystal to be used above the Curie point. Even if the QCM is used at room temperature after this thermal treatment, the QCM does not work at all because of the irreversible loss of the quartz piezoelectric properties. Thus, it is impossible to use quartz crystal microbalances at room temperature after a high-temperature treatment.

A new material, gallium orthophosphate $GaPO_4$ is a quartz structure analogue, Si atoms being replaced by Ga and P atoms in the quartz structure. At first sight, $GaPO_4$ shows very outstanding thermal properties, as it can be used up to a Curie transition temperature of 930 °C.

Despite its thermal properties, very few devices based on $GaPO_4$ working at high temperature have been described. Thanner et al.[22] have studied a high-temperature evaporation phenomenon on a $GaPO_4$ resonator for surface self-cleaning operation. Elam and Pellin[23] have also demonstrated that $GaPO_4$ can be used for growth monitoring of Al_2O_3 and TiO_2 up to 450 °C during atomic layer deposition (ALD).

The aim of this paper is to demonstrate the potential use of $GaPO_4$ crystals for applications using the microbalance technique even when the device has been heated beyond the Curie point of the classical quartz resonators. The dissolution of a thin oxide film obtained from a high temperature treatment of a metallic hydroxide layer was analyzed by using this new microbalance concept. In a first step, the $GaPO_4$ microbalance was calibrated by using an electrochemical copper deposition.[24,25] The influence of the high temperature on the frequency/mass coefficient K_S was examined. These outstanding features were exploited for a dissolution experiment of CeO_2 deposit, produced by an electrochemical method and a thermal treatment at 700 °C. The dissolution rate was successfully measured in different operating conditions for a nitric acid medium containing hydrogen peroxide.

EXPERIMENTAL SECTION

$GaPO_4$ Crystals. The resonators y-11.1°-cut $GaPO_4$ crystals were provided by Piezocryst (Austria). The crystal type R-30 is optimized for use in thin film deposition at high temperature, and the manufacturer guarantees precise measurements up to 800 °C. The resonant frequency is around 5.8 MHz and uses the fundamental thickness shear mode. The crystal has a diameter of 13.97 mm and a thickness of 0.2 mm. Platinum keyhole electrodes were deposited by evaporation techniques, on both sides of the crystal with a titanium adhesion sublayer. The area of the platinum electrode is 0.44 cm^2 (electrode diameter = 0.7 cm). A bevel was made on the resonator in order to obtain a flat polished area at the center of the resonator. In order to use the resonator in liquid medium, a fixed support was designed where the $GaPO_4$ crystal is mounted on a printed circuit board where the electrical contacts are assured by silver paint and where insulation is guaranteed by silicone rubber. In parallel, a removable holder composed of flat-nose alligator clips delivered by the manufacturer were used to measure characteristic parameters like the motional resistance or the resonance frequency of the crystal before thermal treatment because the fixed support and its electrical contacts cannot resist such temperature.

Network Analyzer. Before and after a thermal treatment, $GaPO_4$ crystals were characterized by means of a network analyzer HP4194A to check the piezoelectric response of the crystals. The electrical resonator admittance, $Y_{exp}(\omega)$, was measured around the resonant frequency. The apparatus was driven by a lab-made software, and a fitting program allows the Butterworth−Van Dyke (BVD) equivalent circuit parameters to be obtained.

Microbalance Measurement. For the copper calibrations and the dissolution experiments, the $GaPO_4$ resonator was associated with a lab-made electronic oscillator, adapted to the $GaPO_4$ resonance frequency.[26] The final experimental setup was built by coupling the homemade $GaPO_4$ microbalance with a frequency counter (Philips PM6685) in order to follow the microbalance frequency changes during copper deposition or oxide dissolution.

Copper Electrochemical Deposition. The calibration was performed under galvanostatic copper deposition at various current intensities of 4, 5, and 6 mA, corresponding to current densities of 9, 11.4, and 13.6 mA cm^{-2}, respectively, flowing between the $GaPO_4$ electrode and a platinum wire. The electroplating solution was made with 0.5 M H_2SO_4 and 0.5 M $CuSO_4$. For this range of current densities ($j < 20$ mA cm^{-2}) and with this electrolyte, the yield of deposition is considered to be 100%, the hydrogen evolution being neglected.[24] The copper ion is locally reduced to Cu on the electrode according to eq 1:

$$Cu^{2+} + 2e^- \rightarrow Cu \quad (1)$$

Consequently, the electroplating kinetics depends on the chosen current density. The copper mass, Δm_F, is proportional to the current density as Δm_F can be estimated through the Faraday law. With the choice of different current densities and by plotting Δf versus Δm_F, the experimental mass/frequency sensitivity coefficient can be estimated.

Heat Treatment. High-temperature treatments were performed in a controlled temperature furnace (Nabertherm C42) where the temperature is measured with a thermocouple. For the calibration, before each microbalance measurement, the uncovered resonators were heated up to 600 °C with a temperature ramp of 5 °C/min and left 2 h at 600 °C under inert argon atmosphere.

(20) Rahtu, A.; Ritala, M. *Appl. Phys. Lett.* **2002**, *80* (3), 521.
(21) Gabrielli, C.; Perrot, H.; Rousseau, P.; Belghazi, A.; Chevrot, T.; Colin, J.-M.; Simonet, C. *Rev. Sci. Instrum.* **2005**, *76*, 124102.
(22) Thanner, H.; Krempl, P. W.; Selic, R.; Wallnöfer, W.; Worsch, P. M. *J. Therm. Anal. Calorim.* **2003**, *71*, 53.
(23) Elam, J. W.; Pellin, M. J. *Anal. Chem.* **2005**, *77*, 3531.
(24) Gabrielli, C.; Keddam, M.; Torresi, R. *J. Electrochem. Soc.* **1991**, *138*, 2657.
(25) Bizet, K.; Gabrielli, C.; Perrot, H. *Appl. Biochem. Biotechnol.* **2000**, *89*, 139.
(26) Ehahoun, H.; Gabrielli, C.; Keddam, M.; Perrot, H.; Rousseau, P. *Anal. Chem.* **2002**, *74*, 1119–1127.

Film Formation. First of all, a precipitate of hydrous cerium oxide film $Ce(OH)_4$ was obtained on the platinum electrode of the $GaPO_4$ microbalance using a cathodic deposition method.[27−29] The deposition was obtained electrochemically with a classical three electrode cell: the working electrode was the platinum layer deposited on the $GaPO_4$ resonator, the counter electrode was a large platinum wire, and the reference electrode was a saturated calomel reference electrode (SCE-Radiometer Analytical). A cathodic potential of −0.6 V/SCE was then applied between the electrodes with an Autolab PGSTAT30 potentiostat. This potential corresponds to the reduction process of dissolved oxygen. A homogeneous deposit of the ceria precursor, a hydrous oxide $Ce(OH)_4$, which can also be defined as $CeO_2 \cdot nH_2O$, is then thermally treated at 700 °C under an air atmosphere following the same ramp as previously to form a homogeneous layer of cerium oxide.

Dissolution Experiments. Cerium dissolution experiments were performed with a mixture of HNO_3 and 0.5 M H_2O_2. Different HNO_3 concentrations were studied: 2, 3, 4, and 5 mol L^{-1}. The dissolution experiments took place in a 20 mL cell at room temperature, and the frequency of the resonator was followed during the dissolution of the deposit.

X-ray Diffraction Experiments. CeO_2 powder was analyzed by X-ray diffraction (XRD) with a classical powder diffractometer (D8 Advance Bruker) with a copper anticathode in Bragg−Brentano $\theta-2\theta$ geometry and a Bruker Lynx Eye detector. The XRD diagram was obtained in the 10−80° 2θ range, and intensities were measured at an interval of 2θ equal to 0.02° and 31 s counting time per step with a rotation of the sample. Phase identification was finally made using the EVA software and the ICDD database (JCPDS 34-0394 CeO_2). The powder used for the XRD was prepared by the same electrochemical deposition technique. In this case, the thin film was deposited on a large platinum cylinder by the cathodic deposition technique at a potential of −0.6 V/SCE. The working electrode was then scratched for obtaining the powder samples. The powder was spread on a low-background sample holder (single Si crystal).

SEM Observations. The microstructure of the CeO_2 thin films was observed by scanning electron microscopy (SEM) with a JEOL 5600LV device using the secondary electron mode.

Reagents. All reagents were analytical grade reagents. $CuSO_4 \cdot 5H_2O$ (PROLABO) and H_2SO_4 95% (Prolabo, R.P. Normapur) were used for the calibration. For the preparation of the cerium deposition, cerium nitrate hexahydrate $Ce(NO_3)_3 \cdot 6H_2O$ (Fisher Scientific) was prepared in distilled water at a concentration of 0.05 M. Dissolution solutions were realized with HNO_3 (68%, VWR) and H_2O_2 (30 vol %, Carlo Erba). All chemicals used were reagent grade, and deionized water was used in all the experiments.

(27) Switzer, J. A. *Am. Ceram. Soc. Bull.* **1988**, *66*, 1521.
(28) Aldykiewicz, A. J.; Davenport, A. J.; Isaacs, H. S. *J. Electrochem. Soc.* **1996**, *143*, 147.
(29) Golden, T. D.; Wang, A. Q. *J. Electrochem. Soc.* **2003**, *150*, C621–C624.
(30) Rodriguez-Pardo, L.; Farina, J.; Gabrielli, C.; Perrot, H.; Brendel, R. *Sens. Actuators, B* **2004**, *103*, 318–324.
(31) Rodriguez-Pardo, L.; Farina, J.; Gabrielli, C.; Perrot, H.; Brendel, R. *IEEE Sens. J.* **2005**, *5*, 1251–1257.
(32) Kanazawa, K. K.; Gordon, J. G. *Anal. Chim. Acta* **1985**, *175*, 99.

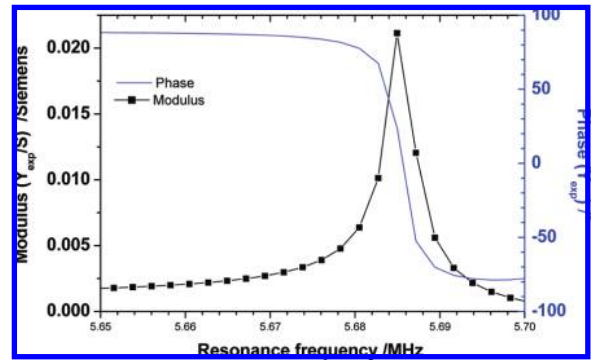

Figure 1. Bode representation of the phase and the modulus of a $GaPO_4$ thickness shear resonator oscillating in water at room temperature after an annealing at 600 °C (T = 22 °C, thickness = 0.2 mm).

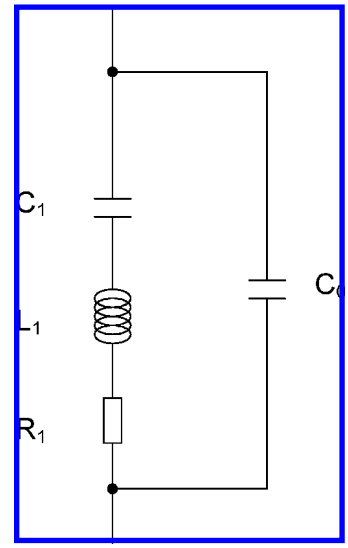

Figure 2. Butterworth−Van Dyke (BVD) equivalent circuit of a piezoelectric resonator. C_0 is the capacity of the crystal, R_1 is the resistance, L_1 is the inductance, and C_1 is the capacity of the motional arm.

Preliminary Validation of the $GaPO_4$ Microbalance. *Influence of High-Temperature Treatments on the Piezoelectric Parameters.* Figure 1 shows the electrical admittance of a $GaPO_4$ thickness shear resonator using the Bode representation. The resonator was mounted in a standard microbalance holder for measuring the resonance behavior in water at room temperature. The main resonance frequency is around 5.68 MHz.

The resonator response can be modeled through a classical equivalent circuit where the series resonant frequency, f_S, and the mechanical quality factor Q, defined as follows, are the main parameters:

$$Q = \frac{2\pi L_1 f_S}{R_1} \tag{2}$$

where L_1 is the inductance and R_1 is the resistance of the motional arm of the Butterworth−Van-Dyke (BVD) equivalent circuit of the resonator (as shown in Figure 2). f_S, the series resonant frequency, is the value which cancels the imaginary part of the dynamic branch of the electrical admittance.

Table 1. Main Parameters R_1, f_S, and Q of a 5.8 MHz $GaPO_4$ in Different Temperature Conditions and with Different Holders

	before annealing 25 °C removable holder in air	after annealing 600 °C during 2 h removable holder in air	after annealing 600 °C during 2 h fixed holder in air	after annealing 600 °C during 2 h fixed holder in water
R_1	5 Ω	10 Ω	9 Ω	53 Ω
f_S	5 737 620Hz	5 737 093Hz	5 736 806Hz	5 735 746Hz
Q	18 900	9 850	11 000	1 900

Q plays a major role in the performance of the resonator, since it measures its quality with respect to the acoustic attenuation. Q is inversely proportional to the disorder and the imperfections of the $GaPO_4$ structure, which means that the higher the quality factor is, the more pure the spectral signal will be and consequently the better the accuracy of the gravimetric measurement.[30,31] Table 1 shows the heat treatment effect but also the influence of the media between air and water on the parameters of the BVD circuit of the same $GaPO_4$ resonator.

As it can be seen, the annealing at 600 °C had only a slight effect on the series resonant frequency which stayed quasi identical before and after the heat treatment. The frequency decrease observed when the microbalance was immersed in water was due to the increase of the viscosity from air to water.[32] The value of 1 kHz is a typical frequency variation when the device is dipped into water. The resistance R_1 also kept a practically constant value around few ohms in air and increased in a liquid environment. Q decreased between a nonheated and a heat-treated resonator, which can be explained by a decrease of the stability of the $GaPO_4$ structure. According to Ellam and Pellin,[23] while the quartz piezoelectric constant Q begins to drop at 300 °C and reaches zero at the Curie point of 573 °C due to a phase transition, the $GaPO_4$ piezoelectric constant remains nearly constant up to 970 °C. So $GaPO_4$ crystals should allow experiments at high temperatures to be performed. However, even if the experiments are performed at room temperature, the accuracy of the gravimetric measurements will be lower after a high-temperature treatment as the accuracy is inversely proportional to the quality factor.[30,31]

With the use of the same $GaPO_4$ and quartz resonators, Figure 3 shows the evolutions of R_1 and Q values after successive annealings at different temperatures from ambient to 700 °C. A different behavior is obtained between the quartz and the $GaPO_4$. The quartz resistance increases rapidly by 2 decades from room temperature to 500 °C instead of the relatively stable resistance of the $GaPO_4$.

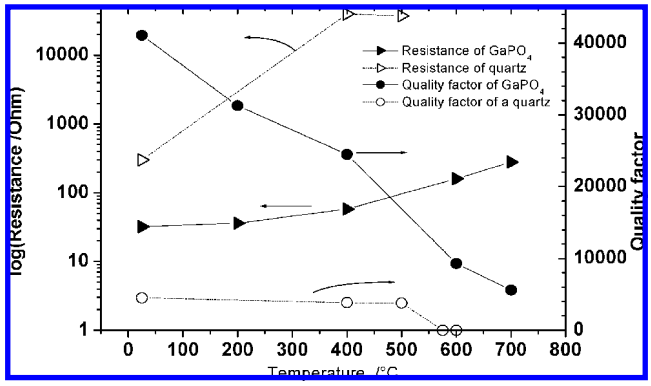

Figure 3. Comparison of the values of the quality factor Q and the resistance R_1 in air at T = 20 °C with the removable holder as a function of the annealing temperature between a 6 MHz quartz and a 5.8 MHz $GaPO_4$ resonator: T = 25, 200, 400, 500, 600, and 700 °C.

The Q factor is very sensitive to the structural disorder. When the annealing temperature increases, the Q factor of the quartz decreases down to 0 at the Curie temperature of 573 °C. The decrease of the Q factor of the $GaPO_4$ is stronger, but after five annealings of the $GaPO_4$ resonator, the Q factor is still higher than those of the quartz crystal. Figure 3 illustrates the better resistance of the $GaPO_4$ crystal to thermal treatments. Consequently, with the comparison of the key properties at high temperatures of both SiO_2 and $GaPO_4$, it is obvious that $GaPO_4$ shows a significantly higher operational temperature limit than quartz.

Effect of the Annealing Temperature on the Copper Calibration of the $GaPO_4$ Microbalance. The microbalance technique is founded on the Sauerbrey equation[3] which describes the resonance frequency response Δf, given by the microbalance device, to an added or removed mass Δm. The equation is described by eq 3:

$$\Delta f = -K_S^{TH}\Delta m \tag{3}$$

where Δf is the measured shift in frequency (Hz) and Δm is the mass change per area unit. The sensitivity factor K_S is the key parameter of the microbalance and is theoretically related to the fundamental resonance frequency of the resonator, as given in eq 4:

$$K_S^{TH} = \frac{2nf_0^2}{\sqrt{\rho\mu}} \quad [\text{in Hz cm}^2\,\text{g}^{-1}] \tag{4}$$

where n is the overtone number (n = 1 in our case), μ is the shear modulus of $GaPO_4$ (2.147×10^{11} g s^{-2} cm^{-1}), ρ is the $GaPO_4$ density (3.570 g cm^{-3}), and f_0 is the fundamental crystal frequency (around 5.8 MHz in air).

The key point to validate the good behavior of this new microbalance was to compare the theoretical value, K_S^{TH}, of the mass/frequency sensitivity coefficient to an experimental one estimated through copper electrogeneration, K_S^{EXP}. More specifically, in order to develop the use of $GaPO_4$ for our measurements, this experimental sensitivity coefficient, K_S^{EXP}, was determined before and after heat treatment in order to determine the temperature effects on the sensitivity of the resonator. The microbalance calibration was carried out in the case of homogeneous mass changes by using copper electrodeposition, as described in an earlier published reference.[25] The K_S^{EXP} coefficient can be calculated through the following equation:

$$K_S^{EXP} = -\left(\frac{\Delta f}{\Delta t}\right)\left(\frac{\Delta t}{\Delta m_F} S\right) \quad (5)$$

in which $((\Delta f)/(\Delta t))$ is the frequency evolution with respect to time recorded with the frequency counter, i.e., the slope of the microbalance measurement, and $((\Delta m_F)/(\Delta t))$ is the added mass on the active surface S (cm^2) of the resonator calculated through the Faraday law:

$$\Delta m_F = \frac{i\Delta t}{2F} M_{Cu} \quad (6)$$

in which i is the imposed current intensity, F is the Faraday number, and M_{Cu} is the copper atomic weight.

$$K_S^{EXP} = -\left(\frac{\Delta f}{\Delta t}\right)\frac{2FS}{iM_{Cu}} \quad (7)$$

The $GaPO_4$ sensitivity factors without and with annealing at 600 °C were experimentally compared. The frequency change, Δf, was recorded with respect to time during the electroplating of copper at different currents at 20 °C.

Figure 4 shows the typical calibration plot for the $GaPO_4$ crystal response without annealing at three different current densities. A linear trend is expected for a thin and rigid film deposition, uniformly distributed over the active area. It can be seen in Figure 5 that a linear change was also observed between time and frequencies even after a heat treatment at 600 °C of the $GaPO_4$ resonator. Moreover, in Table 2 there is neither at room temperature nor after a thermal treatment a significant change of the sensitivity factors K_S^{EXP} with the current density. The values of the theoretical, K_S^{TH} (7.92×10^7 Hz cm^{-1} g^{-1}) and the experimental K_S^{EXP} values were of the same order. It should be noted that the same deviation exists for a classical 6 MHz quartz resonator with a K_S^{TH} value of 8.14×10^7 Hz g^{-1} cm^2 and an experimental value of 7.49×10^7 Hz g^{-1} cm^2. These deviations can be due to the geometry of the resonator, in particular the size of the electrode.[25] We can also observe that the sensitivity factors of a quartz and a $GaPO_4$ are almost similar. These copper calibrations of the $GaPO_4$ microbalance prove that practically the high-temperature treatment does not have an impact on the mass/frequency sensitivity coefficient.

RESULTS AND DISCUSSION

The formation of cerium oxide begins by the precipitation of $Ce(OH)_4$ at the Pt electrode of the $GaPO_4$ crystal microbalance

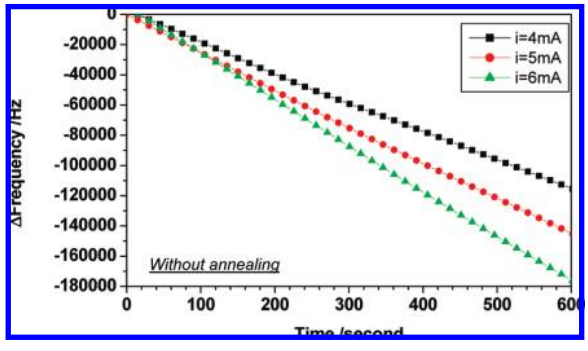

Figure 4. Calibration of the $GaPO_4$ microbalance by copper electrodeposition for different current intensities at room temperature without a high-temperature treatment; $T = 20$ °C, electrode area = 0.44 cm^2, deposition solution: $[H_2SO_4] = 0.5$ M $[CuSO_4] = 0.5$ M.

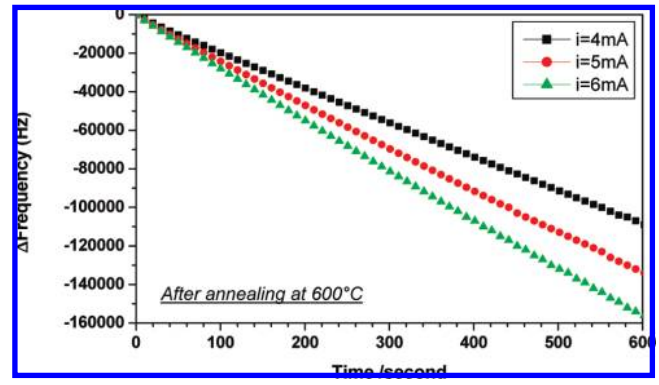

Figure 5. Calibration of the $GaPO_4$ microbalance at room temperature by copper electrodeposition for different current intensities after a high-temperature treatment at 600 °C; $T = 20$ °C, electrode area = 0.44 cm^2, deposition solution: $[H_2SO_4] = 0.5$ M, $[CuSO_4] = 0.5$ M.

Table 2. Comparison of the Sensitivity Factor at Different Current Densities: *i*= 4, 5, and 6 mA with and without Annealing at 600°C

current density/mA	K_S/Hz cm^2 g^{-1} without annealing	K_S/Hz cm^2 g^{-1} with annealing at 600 °C
$i = 4$ mA	6.51×10^7	6.88×10^7
$i = 5$ mA	6.42×10^7	6.56×10^7
$i = 6$ mA	6.68×10^7	6.29×10^7
average K_s	6.5×10^7	6.6×10^7

by an electrochemical method using OH^- production by electrolysis. The oxygen reduction reaction at $E = -0.6$ V/SCE generates *in situ* hydroxyl ions at the interface electrode/solution, where the local pH is consequently increased.

$$O_2 + 2H_2O + 2e^- \leftrightarrow H_2O_2 + 2OH^- \quad (8)$$

$$H_2O_2 + 2e^- \rightarrow 2OH^- \quad (9)$$

The overall reaction is given by

$$O_2 + 2H_2O + 4e^- \rightarrow 4OH^- \quad (10)$$

The reactions for precipitation and film formation are thought to be

$$Ce^{3+} + 3OH^- \rightarrow Ce(OH)_3 \quad (11)$$

$$Ce^{3+} + OH^- + \frac{1}{2}H_2O_2 \rightarrow Ce(OH)_2^{2+} \quad (12)$$

$$Ce(OH)_2^{2+} + 2OH^- \rightarrow Ce(OH)_4 \quad (13)$$

Hydrogen peroxide, produced *in situ* by eq 8, can achieve the oxidation of Ce(III) to Ce(IV).[33,34] Moreover, oxidation of $Ce(OH)_3$ also occurs in air at room temperature to form $Ce(OH)_4$. The $Ce(OH)_4$ film was then thermally treated at 700 °C under air atmosphere to obtain a CeO_2 film.

(33) Scholes, F. H.; Hughes, A. E.; Hardin, S. G.; Lynch, P.; Miller, P. R. *Chem. Mater.* **2007**, *19*, 2321–2328.
(34) Wang, A. Q.; Golden, T. D. *J. Electrochem. Soc.* **2003**, *150*, C616–C620.

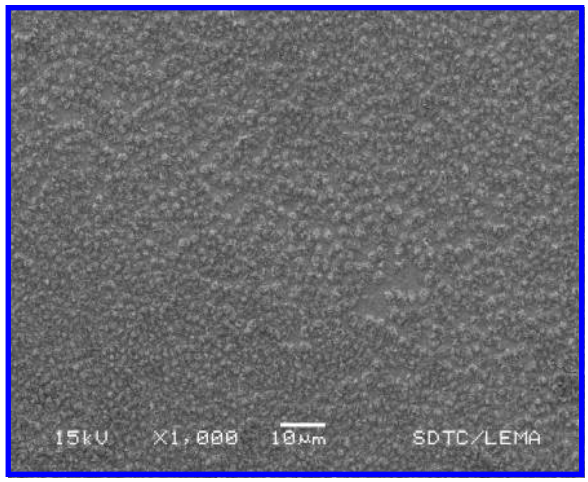

Figure 6. SEM image of CeO_2 film deposited on a platinum electrode of a $GaPO_4$ resonator from an aqueous solution of 0.05 M $Ce(NO_3)_3$. Deposition at −0.6 V/SCE and heat treatment at 700 °C.

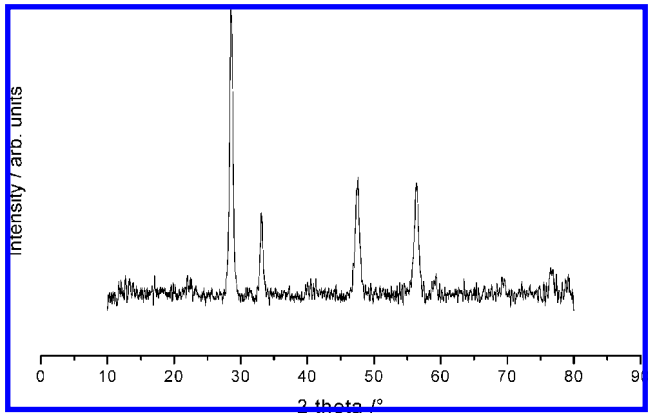

Figure 7. XRD patterns of CeO_2 powders after a high-temperature treatment at 700 °C.

SEM observations of CeO_2 obtained after an annealing at 700 °C of $Ce(OH)_4$ reveal that the films are almost uniform and adherent at the electrode. Figure 6 shows the surface morphology of cerium oxide precipitated by a cathodic deposition at −0.6 V/SCE after 23 min in an aqueous solution containing 0.05 M $Ce(NO_3)_3$. Spherical particles of $Ce(OH)_4$ became more compact after the annealing at high temperature and show a lamellar morphology similar to gypsum flowers. The particles diameters are around 2 μm.

Figure 7 presents the XRD diagram of the powder from the thin film. XRD pattern obtained is typical of cerium oxide CeO_2 with the cubic fluorite structure as it is reported in the literature (JCPDS Index Card 00-034-0394). In fact, the well-defined diffraction peaks correspond to the (111), (200), (220), and (311) ceria crystallographic planes. No diffraction lines associated with Ce(III) oxide are present.

Cerium oxide dissolution experiments with various HNO_3 concentrations were carried out in order to measure the dissolution rate as a function of $[H^+]$. In fact, previous studies[35] have shown that for many minerals the acid-promoted dissolution rate R_H is proportional to the hydrogen concentration and obeys the empirical rate law:

$$R_H = k[H^+]^n \quad (14)$$

Here, the dissolution reaction is thought to be

$$CeO_2 + 4H^+ \leftrightarrows Ce^{4+} + 2H_2O \quad \Delta rG^\circ = 40.1\ \text{kJ mol}^{-1} \quad (15)$$

The weight loss occurring when the CeO_2 film was immersed in oxidizing solutions was followed by measuring the frequency change of the $GaPO_4$ crystal microbalance. Figure 8 shows that the dissolution rate in a pure HNO_3 solution was very slow and the cerium oxide film was not dissolved. That is due to the fact that cerium oxide CeO_2 is a refractory oxide which dissolves very slowly even in 7 mol L^{-1} HNO_3.[10] Without a redox state change, the dissolution reaction of CeO_2 in nitric acid solution is not thermodynamically favorable ($\Delta G^\circ > 0$). Therefore, a reducing agent (Fe(II), HI, or H_2O_2) must be added to the acidic medium in order to pass CeO_2 in solution.[11] A change in the oxidation state will affect the solubility of the metal oxide. Stumm and Wollast[35] have suggested that the reduced metal−oxygen bond has a larger lability than the nonreduced metal−oxygen bond. Cerium reduction with H_2O_2 can be written as

$$CeO_{2(s)} + 3H^+ + \frac{1}{2}H_2O_2 \leftrightarrows Ce^{3+} + 2H_2O + \frac{1}{2}O_2 \quad \Delta rG^\circ = -125.9\ \text{kJ mol}^{-1} \quad (16)$$

In the presence of 0.5 M H_2O_2 at room temperature, four HNO_3 concentrations were considered: 2, 3, 4, and 5 mol L^{-1}. With the use of the dissociation constant $K_{a(HNO_3)}$ of nitric acid,[36] the free acidity concentration $[H^+]$ can be calculated in strong nitric acid medium: 1.82, 2.63, 3.39, and 4.11 M, respectively.

$$HNO_3 + H_2O \rightarrow H_3O^+ + NO_3^- \quad \log(K_a) = -1.30 \quad (17)$$

Figure 8 shows the effect of H^+ concentration on the CeO_2 dissolution. The dissolution rate of CeO_2 increases with the increase of the acid concentration. The dissolution rates were estimated by using a linear fitting of the initial mass change

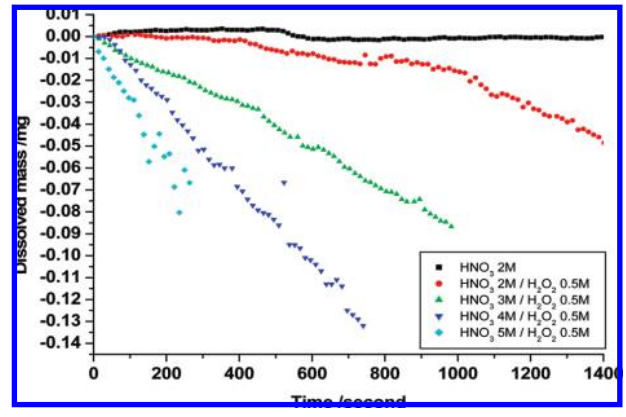

Figure 8. Dissolution of CeO_2 obtained at different HNO_3 concentrations (2, 3, 4, and 5 M), at $T = 25$ °C and $[H_2O_2] = 0.5$ M.

(35) Stumm, W.; Wollast, R. *Rev. Geophys.* **1990**, *28*, 1.

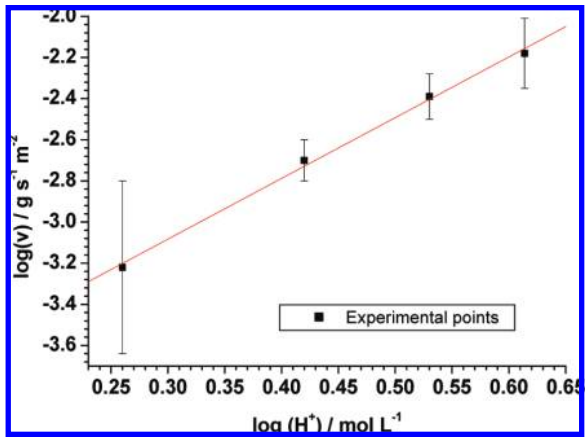

Figure 9. Change of the CeO_2 dissolution rate with respect to pH: $\log(V) = k \log([H^+])$ at $T = 25$ °C.

recorded by the $GaPO_4$ microbalance, thanks to the Sauerbrey's equation, over the time and for each hydrogen concentrations $[H^+]$.

Figure 9 shows the log of the dissolution rate vs $\log[H^+]$ at 25 °C, and a linear trend was observed. The reaction order with respect to $[H^+]$ was directly calculated from the slope of the line shown in Figure 8, and a value of $n = (2.9 \pm 0.2)$ was obtained. That means that the dissolution kinetic was proportional to the 2.9 power of $[H^+]$.

However, for a general reaction such as

$$v_1A_1 + v_2A_2 + \ldots \Leftrightarrow v'_1A'_1 + v'_2A'_2 + \ldots \quad (18)$$

Van't Hoff theory gives the rate v of a chemical reaction under the form

$$v = k \prod_i [A_i]^{v_i} \quad (19)$$

According to eq 16, if the reaction obeys the Van't Hoff law, the rate law should be written as

$$v = k'[H^+]^3 \quad (20)$$

For the cerium dissolution, the partial rate order n with respect to $[H^+]$ is very close to 3, which could point out that a law similar to the Van't Hoff theory governs the CeO_2 dissolution. Moreover, that means also that the reduction of Ce(IV) to Ce(III) is the rate determining step of the dissolution reaction.

The reaction order obtained here is quite different from the typical coefficient seen in the literature, classically ranging between 0.4 and 1.[37,38] Nevertheless, these results about cerium oxide dissolution were carried out in very different experimental conditions. Indeed the experiments found in the literature correspond to commercial CeO_2 powders, whereas in our experiments, thin CeO_2 films were made electrochemically from cerium nitrate followed by annealing. Moreover, times of dissolution were also different. In our case, we measured the initial dissolution rate during the first 20 min whereas several hours of dissolution were studied in previous references. It is well-known that the kinetic related to the oxide dissolution is influenced by the sample preparation method. Therefore, it is quite difficult to compare our data with the results given in the literature. However, when the dissolution is complicated with hydration, redox reactions, or complex formation, the formal order of the reaction takes on different values.[38]

CONCLUSIONS

This study demonstrated the potential use of $GaPO_4$ crystal as a resonator for the microbalance technique. The property of this crystal allows gravimetric experiments to be carried out after higher temperature treatments as the $GaPO_4$ resonator remains operational contrarily to the quartz. It opens also great perspectives for gravimetric measurements performed at high temperatures. However, even if the sensitivity coefficient does not depend on the temperature treatments, the accuracy of the measurement will be decayed.

The $GaPO_4$ crystal was particularly useful for the study of cerium thin film dissolution, in which the manufacturing protocol imposed a high-temperature treatment of the thin hydroxide layer at 700 °C. It was proven by the $GaPO_4$ microbalance that the free acidity concentration had a great influence on the dissolution rate of cerium oxide. In addition, in the presence of hydrogen peroxide, the partial rate order is in agreement with the stoichiometric coefficient of the hydrogen ion in the dissolution equation. A kinetic law similar to Van't Hoff theory seems to govern the dissolution reaction of cerium oxide. In this case, the rate determining step of CeO_2 dissolution could be controlled by the reduction reaction of Ce(IV) to Ce(III). This hypothesis has to be confirmed by future experiments. More research about the $GaPO_4$ microbalance is in progress in our laboratory in order to study the influence of the thermal treatment of the thin layer of oxide material in regard to it's refractory behavior.

ACKNOWLEDGMENT

The authors gratefully acknowledge AREVA for its financial support. The authors also thank Mr. G. Folcher (CNRS) for the $GaPO_4$ electrodes fabrication and Mr. D. Rose (CNRS) for the microbalance oscillator. The authors are grateful to S. Caron (DEN/MAR/DTEC/SDTC/LEMA) for the SEM observation.

Received for review April 17, 2009. Accepted June 1, 2009.

AC900826U

(36) Davis, W., Jr; De Bruin, H. J. *J. Inorg. Nucl. Chem.* **1964**, *26*, 1069–1083.
(37) Terry, B. *Hydrometallurgy* **1983**, *11*, 315–344.
(38) Gorichev, I. G.; Kipriyanov, N. A. *Russ. Chem. Rev.* **1984**, *53*, 11.